Supporting Information for: Solubility of Carbon Dioxide, Hydrogen Sulfide, Methane, and Nitrogen in Monoethylene Glycol; Experiments and Molecular Simulation

Noura Dawass,[†] Ricardo R. Wanderley,[‡] Mahinder Ramdin,[†] Othonas A. Moultos,[†] Hanna K. Knuutila,[‡] and Thijs J. H. Vlugt[*,†]

[†]*Engineering Thermodynamics, Process & Energy Department, Faculty of Mechanical, Maritime and Materials Engineering, Delft University of Technology, Leeghwaterstraat 39, 2628CB, Delft, The Netherlands*

[‡]*Department of Chemical Engineering, Norwegian University of Science and Technology, 7034 Trondheim, Norway*

E-mail: t.j.h.vlugt@tudelft.nl

In this Supporting Information, we show the derivation for the expression to compute the saturated vapor pressure of a pure component simulated using Continuous Fractional Component Monte Carlo simulations (CFCMC). Also, we provide force field parameters of all molecules simulated in this work. We describe how expanded uncertainties of the experimental data are computed. Tabulated experimental data of the solubilities of CO_2, CH_4, H_2S, and N_2 in monoethylene glycol (MEG) are provided as well as tables of the solubilities of CO_2, CH_4, H_2S, and N_2 in MEG from MC simulations.

Force field parameters

Force field for MEG

The TraPPE force field[1] was used to model MEG. In this force field, bonded angle-bending interactions are described using a harmonic potential:

$$u_{\text{bend}}(\theta) = \frac{K_\theta}{2}(\theta - \theta_{\text{eq}})^2 \tag{S.1}$$

where K_θ is the bond bending constant, θ is the angle between two bonds and θ_{eq} is the equilibrium angle. For dihedrals, torsion interaction potential of the type TraPPE is used:[2]

$$u_{\text{torsion}}(\phi) = c_o + c_1[1 + \cos\phi] + c_2[1 - \cos 2\phi] + c_3[1 + \cos 3\phi] \tag{S.2}$$

where ϕ is the torsion angle. Parameters for non-bonded interactions are provided in Table S1. For unlike interactions, the Lorentz-Berthelot combining rules are used.[3,4] An extra repulsive LJ term is computed for interactions between a hydroxyl hydrogen and an oxygen atom separated by four bonds:[1]

$$u_{\text{repulsive}}(r_{ij}) = \frac{a_{\text{alcohol}}}{r_{ij}^{12}} \tag{S.3}$$

where $a_{\text{alcohol}}/k_{\text{B}}$ equals to 7.5x10^7 K Å^{12} for MEG. Bonds lengths, bending interactions, and dihedrals are provided in Table S1.

Table S1: Force field parameters for MEG taken from the TraPPE force field.[1] Bond-bending angles are represented by a harmonic potential. A TraPPE torsion potential is used for dihedrals.[2]

Non-bonded interactions			
	CH_2	O	H
$\epsilon_{ii}/k_B/[K]$	46	93	0
$\sigma_{ii}/[Å]$	3.95	3.02	0.00
$q_i/[e]$	0.265	−0.700	0.435

Bond lengths	
Bond	$r_{ij}/[Å]$
CH_2–CH_2	1.54
CH_2–OH	1.43
O–H	0.945

Bond-bending Angles (Eq. (S.1))		
Angle	θ	$K_\theta/k_B/[K/rad^2]$
CH_2–CH_2–OH	109.47°	50400
CH_2–O–H	108.5°	55400

Dihedrals (Eq. (S.2))				
Torsion	c_0/k_B /[K]	c_1/k_B /[K]	c_2/k_B /[K]	c_3/k_B /[K]
CH_2–CH_2–O–H	0	209.82	−29.17	187.93
O–CH_2–CH_2–O	503.24	0	−251.62	1006.47

Force field for gases

Table S2: Force field parameters for CH_4 used in this work taken from the TraPPE.[2] For unlike interactions, the Lorentz-Berthelot combining rules are used.[3,4]

Parameter	CH_4
ϵ_{ii}/k_B /[K]	148
σ_{ii}/[Å]	3.73
$q_i/[e]$	0.00

Table S3: Force field parameters for N_2 used in this work taken from the TraPPE.[5] The force field includes a pseudo atom M, placed in between the two nitrogen atom. Bonds between atoms are rigid. For unlike interactions, the Lorentz-Berthelot combining rules are used.[3,4]

Non-bonded interactions		
	N	M
$\epsilon_{ii}/k_{\mathrm{B}}$ /[K]	36	0.00
σ_{ii}/[Å]	3.310	0.00
$q_i/[e]$	−0.482	0.964
Bond lengths		
Bond	r_{ij}/[Å]	
N–N	1.10	
N–M	0.55	

Table S4: Force field parameters for CO_2 used in this work taken from the TraPPE.[5] All bonds are rigid. For unlike interactions, the Lorentz-Berthelot combining rules are used.[3,4]

Non-bonded interactions		
	C	O
ϵ_{ii}/k_B /[K]	27.00	79.00
σ_{ii}/[Å]	2.80	3.05
$q_i/[e]$	0.70	−0.35
Bond lengths		
Bond	r_{ij}/[Å]	
C–O	1.16	

Table S5: Force field parameters for H_2S used in this work taken from the TraPPE.[6] The force field includes a pseudo atom M that that is separated from the S atom by r_{S-M} and placed toward the H atoms along the H–S–H angle bisector. All bonds are rigid. For unlike interactions, the Lorentz-Berthelot combining rules are used.[3,4]

Non-bonded interactions			
	S	H	M
ϵ_{ii}/k_B /[K]	122	50	0.00
σ_{ii}/[Å]	3.6	2.5	0.00
$q_i/[e]$	0.00	0.00	−0.42
Bond lengths			
Bond	r_{ij}/[Å]		
S–H	1.34		
S–M	0.3		

Table S6: Force field parameters for the force field H_2S-KL.[7] The force field includes a pseudo atom M that is separated from the S atom by r_{S-M} and placed toward the H atoms along the H–S–H angle bisector. All bonds are rigid. For unlike interactions, the Lorentz-Berthelot combining rules are used.[3,4]

Non-bonded interactions			
	S	H	M
ϵ_{ii}/k_B /[K]	250	0	0
σ_{ii}/[Å]	3.73	0.00	0.00
$q_i/[e]$	0.40	0.25	−0.9

Bond lengths	
Bond	r_{ij}/[Å]
S–H	1.34
S–M	0.1862

Computing saturated vapor pressure of pure components from CFCMC simulations

In CFCMC, the excess chemical potential of a component is directly obtained, from which the saturated vapor pressure P^{sat} of that component can be estimated. The chemical potential of the liquid phase of component i equals:

$$\mu^L = \mu^o + k_{\text{B}}T \ln \frac{\rho^{\text{L}}}{\rho^o} + \mu^{\text{ex}} \tag{S.4}$$

where ρ^{L} is the number density and μ^o is the ideal gas chemical potential. Assuming an ideal gas phase, the chemical potential of the saturated vapor equals:

$$\mu^V = \mu^o + k_{\text{B}}T \ln \frac{\rho^{\text{V}}}{\rho^o} \tag{S.5}$$

At equilibrium, the liquid and vapor chemical potentials are equal, which results in the following expression,

$$k_{\text{B}}T \ln \frac{\rho^{\text{V}}}{\rho^{\text{L}}} = \mu^{\text{ex}} \tag{S.6}$$

By assuming an ideal gas phase, the density in the vapor phase can written in terms of the density and excess chemical potential of the liquid,

$$P^{\text{sat}} = k_{\text{B}}T\rho^{\text{L}} \exp\left[\frac{\mu^{\text{ex}}}{k_{\text{B}}T}\right] \tag{S.7}$$

Calculation of Expanded Uncertainties in the Absorption Experiments

The calculation of expanded uncertainties with a 0.95 level of confidence has been performed following the same procedure employed by Skylogianni et al.[8] Skylogianni et al.[8] have obeyed the NIST Requirements for Data Tables, according to which $U(\alpha) = 2.u(\alpha)$. In this equation, $U(\alpha)$ is the expanded uncertainty of loadings with 0.95 level of confidence, and $u(\alpha)$ accounts both for the inherent inaccuracies of loading measurements and for the deviations originating from the repeatability of practical experiments. Therefore, we have:

$$U(\alpha) = 2.u(\alpha) \tag{S.8}$$

$$u^2(\alpha) = u^2_{\text{inh}}(\alpha) + u^2_{\text{rep}}(\alpha) \tag{S.9}$$

The inherent uncertainties of loadings can be calculated by the procedure adopted by Wanderley et al.[9,10] and by Skylogianni et al.[11] For this procedure, one needs to know the confidence intervals of pressure and temperature measurements, as well as the uncertainties of the volumes of each equipment used in the experiment. In our case, pressures are obtained with a confidence of $\sigma(p) = \pm 0.015$ bar and temperatures are obtained with $\sigma(T) = \pm 0.01$ K. The reactor has a volume of 2000 $\pm$ 10 cm^3, while the CO_2 cylinders have an added volume of 4552 $\pm$ 5 cm^3, so that $\sigma(V_{\text{r}}) = \pm 10^{-5}$ m^3 and $\sigma(V_{\text{c}}) = \pm 5x10^{-6}$ m^3. Finally, the uncertainty of mass measurements is given by the accuracy of the scale, $\sigma(m) = \pm 10^{-5}$ kg. The volume of the vapor phase of the reactor is given by subtracting the volume of liquid in the reactor from its total volume. Therefore, one needs to know how much liquid is inside the reactor and its density. If one assumes that the density of the liquid is given with great accuracy when compared to the inaccuracies of all other measurements, the expression below (Eq. S12) can be used to evaluate the uncertainty of the volume of vapor in the reactor. Notice that, since the mass of ethylene glycol fed to the reactor is evaluated through two

mass measurements (weighting of the ethylene glycol bottle before and after feeding):

$$\sigma(m_{\mathrm{L}}) = 2.\sigma^2(m) \tag{S.10}$$

$$V_{\mathrm{r,V}} = V_{\mathrm{r}} - V_{\mathrm{r,L}} = V_{\mathrm{r}} - \frac{mL}{\rho L} \tag{S.11}$$

$$\sigma^2(V_{\mathrm{r}}, v) = \sigma^2(V_{\mathrm{r}}) + 2.\frac{\sigma^2(m)}{\rho^2 L} \tag{S.12}$$

The number of moles of CO_2 added to the reactor during each injection is given by subtraction of the evaluated number of moles of CO_2 in the cylinder before and after injection. Part of this CO_2 will go to the liquid phase and part will remain in the vapor phase. This can be calculated by the expression below, where $n_{\mathrm{c,i}}$ and $n_{\mathrm{c,f}}$ are the initial and final number of moles in the cylinder respectively and $n_{\mathrm{r,i}}$ and $n_{\mathrm{r,f}}$ are the initial and final number of moles in the vapor phase of the reactor respectively:

$$\Delta n = (n_{\mathrm{c,i}} - n_{\mathrm{c,f}}) - (n_{\mathrm{r,i}} - n_{\mathrm{r,f}}) \tag{S.13}$$

Following the ideal gas law approach, the inherent uncertainty of the loading $\sigma(\Delta n)$ can be evaluated by:

$$\begin{aligned}\sigma^2(\Delta n) = &\left[\frac{\sigma^2(p)}{p_{\mathrm{c,i}}^2} + \frac{\sigma^2(T)}{T_{\mathrm{c,i}}^2} + \frac{\sigma^2(V_{\mathrm{c}})}{V_{\mathrm{c}}^2}\right].n_{\mathrm{c,i}}^2 + \left[\frac{\sigma^2(p)}{p_{\mathrm{c,f}}^2} + \frac{\sigma^2(T)}{T_{\mathrm{c,f}}^2} + \frac{\sigma^2(V_{\mathrm{c}})}{V_{\mathrm{c}}^2}\right].n_{\mathrm{c,f}}^2 + \\ &\left[\frac{\sigma^(p)}{p_{\mathrm{r,i}}^2} + \frac{\sigma^(T)}{T_{\mathrm{r,i}}^2} + \frac{\sigma^2(V_{\mathrm{r,V}})}{V_{\mathrm{r,V}}^2}\right].n_{\mathrm{r,i}}^2 + \left[\frac{\sigma^(p)}{p_{\mathrm{r,f}}^2} + \frac{\sigma^(T)}{T_{\mathrm{r,f}}^2} + \frac{\sigma^2(V_{\mathrm{r,V}})}{V_{\mathrm{r,V}}^2}\right].n_{\mathrm{r,f}}^2\end{aligned} \tag{S.14}$$

The number of mols of ethylene glycol in the reactor is given by the ratio between its mass and its molar mass in kg/mol. Therefore, the inherent uncertainty of the mass of ethylene

glycol in the reactor is given by the expression below:

$$n_{\mathrm{L}} = \frac{m_{\mathrm{L}}}{M_{\mathrm{L}}} \tag{S.15}$$

$$\sigma^2(n_{\mathrm{L}}) = 2.\frac{\sigma^2(m)}{M_L^2} \tag{S.16}$$

The loading obtained with one single injection can be therefore calculated by:

$$\Delta\alpha = \frac{\Delta n}{n_{\mathrm{L}}} \tag{S.17}$$

$$\frac{\sigma^2(\Delta\alpha)}{\Delta\alpha^2} = \frac{\sigma^2(\Delta n)}{\Delta n^2} + \frac{\sigma^2(n_{\mathrm{L}})}{n_{\mathrm{L}}^2} \tag{S.18}$$

Finally, since the total loading is given by the addition of the loadings obtained after each injection, error propagation entails the expression below. This is how we have evaluated and reported the inherent uncertainties of all CO_2 loadings,

$$\alpha = \sum \Delta\alpha \tag{S.19}$$

$$\sigma^2(\alpha) = \sum \sigma^2(\Delta\alpha) \tag{S.20}$$

$$u_{\mathrm{inh}}^2 = \frac{\sigma^2(\alpha)}{\alpha^2} \tag{S.21}$$

In general, this calculation procedure has resulted $u_{\mathrm{inh}} \approx 0.02$ for our experiments, meaning that our experiments result in loadings with inherent inaccuracies of around 2%. However, one must realize that these are *inherent* inaccuracies, i.e. merely a lower boundary estimate of the uncertainties of this procedure. For a proper evaluation of the expanded uncertainty of loadings with a 0.95 level of confidence, one needs repeatability data. The repeatability of our experiments has been evaluated with distinct sets of data obtained in Wanderley et al.[10] for CO_2 solubility in a nonaqueous solvent, N–methyl–2–pyrrolidone + diisopropylamine 10 %wt., at 40 °C . This data, which is presented in Figure S1, has been

produced in the same apparatus as the one employed in the current study, as well as in the same months of the same year.

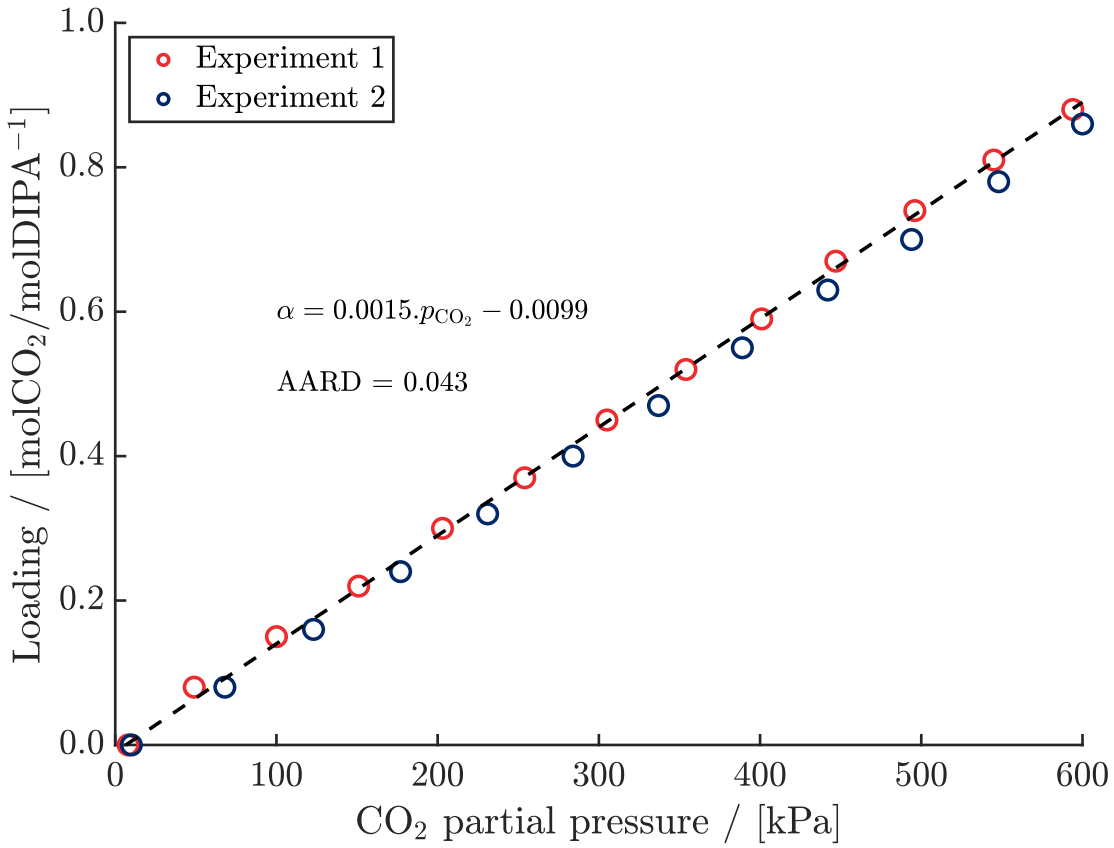

Figure S1: Data obtained by Wanderley et al.[10] used for estimating the repeatability of the experimental procedure for CO_2 solubility in a nonaqueous solvent, N–methyl–2–pyrrolidone + diisopropylamine 10 %wt., at 40 °C.

Since the aforementioned nonaqueous solvent absorbs CO_2 without a chemical reaction, there appears to be a linear relationship between CO_2 loading and CO_2 partial pressure in the solubility measurements shown by Wanderley et al.[10] This fact has been used to perform a linear regression over the sets of data produced by the authors, and to thus estimate the repeatability of the experimental setup as being the same as the AARD calculated over these datasets. This is shown in the expression below. The AARD obtained from this mathematical methodology is AARD = 0.043, meaning that the repeatability of the CO_2

solubility procedure is around 4.3%:

$$u_{\mathrm{rep}}(\alpha) = \frac{1}{N_{\mathrm{exp}}} . \sum \left| \frac{\alpha_{\mathrm{exp}} - \alpha_{\mathrm{corr}}}{\alpha_{\mathrm{exp}}} \right| \tag{S.22}$$

Finally, using the methodology employed by Skylogianni et al.,[8] the expanded uncertainties with a 0.95 level of confidence can be evaluated. Table S7 shows an example of this calculation for the CO_2 solubilities measured at 333.15 K in pure ethylene glycol. One can see that the expanded uncertainties vary between 9% and 11%, being higher at smaller loadings. In fact, roughly the same values can be observed at $T = 353.15$ K and $T = 373.15$ K, as shown in Table S8 and Table S9. In general, therefore, we can safely report that the CO_2 solubility data obtained in this study has expanded uncertainties with a 0.95 level of confidence of approximately $U(\alpha) = 0.1$.

Experimental Data

Table S7: Experimental absorption of CO_2 in pure MEG at $T = 333.15$ K reported in this work.

P /[bar]	Loading /[mol CO_2/mol EG]	$u_{\text{inh}}(\alpha)$	$u(\alpha)$	$U(\alpha)$
0.73 ± 0.02	0.0012	0.029	0.052	0.104
1.36 ± 0.02	0.0021	0.020	0.047	0.095
2.03 ± 0.02	0.0033	0.017	0.046	0.092
2.69 ± 0.02	0.0043	0.016	0.046	0.092
3.35 ± 0.02	0.0052	0.016	0.046	0.092
4.00 ± 0.02	0.0062	0.016	0.046	0.092
4.66 ± 0.02	0.0073	0.016	0.046	0.091
5.31 ± 0.02	0.0084	0.016	0.046	0.091

Table S8: Experimental absorption of CO_2 in pure MEG at $T = 353.15$ K reported in this work.

P /[bar]	Loading /[mol CO_2/mol EG]	$u_{\text{inh}}(\alpha)$	$u(\alpha)$	$U(\alpha)$
0.74 ± 0.02	0.0010	0.034	0.055	0.109
1.45 ± 0.02	0.0020	0.021	0.048	0.095
2.19 ± 0.02	0.0030	0.018	0.046	0.093
2.93 ± 0.02	0.0040	0.018	0.046	0.093
3.67 ± 0.02	0.0050	0.017	0.046	0.093
4.39 ± 0.02	0.0059	0.017	0.046	0.093
5.11 ± 0.02	0.0069	0.017	0.046	0.093
5.83 ± 0.02	0.0079	0.017	0.046	0.093

Table S9: Experimental absorption of CO_2 in pure MEG at $T = 373.15$ K reported in this work.

P /[bar]	Loading /[mol CO_2/mol EG]	$u_{\text{inh}}(\alpha)$	$u(\alpha)$	$U(\alpha)$
0.71 ± 0.02	0.0009	0.036	0.056	0.112
1.50 ± 0.02	0.0018	0.023	0.049	0.098
2.29 ± 0.02	0.0026	0.021	0.048	0.095
3.07 ± 0.02	0.0036	0.019	0.047	0.094
3.84 ± 0.02	0.0046	0.019	0.047	0.094
4.62 ± 0.02	0.0055	0.019	0.047	0.094
5.39 ± 0.02	0.0065	0.019	0.047	0.094

Table S10: Experimental absorption of CO_2 in pure MEG at $T = 373$ K reported in Ref.[12]

P /[bar]	Mole fraction of CH_4
0.76	0.00072
1.29	0.00127
8.02	0.00748
39.5	0.03803
75.1	0.06667

Table S11: Experimental absorption of CH_4 in pure MEG at $T = 373.15$ K reported in Ref.[13]

P /[bar]	Mole fraction of CH_4
17.944	0.0031
38.764	0.0066
59.170	0.0104
81.992	0.0143
112.164	0.0196

Table S12: Experimental absorption of N_2 in pure MEG at $T = 373.15$ K reported in Ref.[12]

P /[bar]	Mole fraction of N_2
16.00	0.0005
49.60	0.0022
98.00	0.0040
152.30	0.0059

Table S13: Experimental absorption of H_2S in pure MEG at $T = 373.15$ K reported in Ref.[14]

P /[bar]	Mole fraction of H_2S
0.0364	0.000152
0.0961	0.00044
0.144	0.000664
1.19	0.005188
5.36	0.02338
12.8	0.05760
28.2	0.133
67.5	0.4650

Simulation results

Table S14: Solubility of CO_2 in pure MEG at $T = 333.15$ K computed from MC simulations reported in this work.

P /[bar]	Loading /[mol CO_2/mol EG]
0.73	0.00166 ± 0.00008
1.36	0.0031 ± 0.0002
2.03	0.0046 ± 0.0002
2.69	0.0063 ± 0.0002
3.35	0.0077 ± 0.0003
4.00	0.0087 ± 0.0004
4.66	0.0107 ± 0.0004
5.31	0.0119 ± 0.0003
8	0.0183 ± 0.0006
10	0.0236 ± 0.0009

Table S15: Solubility of CO_2 in pure MEG at $T = 353.15$ K computed from MC simulations reported in this work.

P /[bar]	Loading /[mol CO_2/mol EG]
0.74	0.00126 ± 0.00008
1.45	0.00253 ± 0.00007
2.19	0.0038 ± 0.0002
2.93	0.0050 ± 0.0001
3.67	0.0063 ± 0.0002
4.39	0.0077 ± 0.0003
5.11	0.0089 ± 0.0003
5.83	0.0100 ± 0.0002
8	0.0134 ± 0.0006
10	0.0174 ± 0.0006

Table S16: Solubility of CO_2 in pure MEG at $T = 373.15$ K computed from MC simulations reported in this work.

P /[bar]	Loading /[mol CO_2/mol EG]
0.71	0.00097 ± 0.00002
1.50	0.00207 ± 0.00007
2.29	0.0032 ± 0.0001
3.07	0.0044 ± 0.0001
3.84	0.0053 ± 0.0001
4.62	0.0065 ± 0.0002
5.39	0.0075 ± 0.0002
8	0.0114 ± 0.0003
10	0.0138 ± 0.0003

Table S17: Solubility of CH_4 in pure MEG at $T = 373.15$ K computed from MC simulations reported in this work.

P /[bar]	Mole fraction of CH_4
1	0.00022 ± 0.00001
2	0.00045 ± 0.00002
4	0.00089 ± 0.00003
6	0.0013 ± 0.0001
8	0.00182 ± 0.00007
10	0.00222 ± 0.00005
17.9	0.0039 ± 0.0001

Table S18: Solubility of H_2S in pure MEG at $T = 373.15$ K computed using MC simulations reported in this work.

P /[bar]	Mole fraction of H_2S (H_2S-TraPPE)	Mole fraction of H_2S (H_2S-K)
1	0.0033 ± 0.0001	0.0058 ± 0.0002
2	0.0066 ± 0.0002	0.0114 ± 0.0002
4	0.0134 ± 0.0003	0.0229 ± 0.0004
6	0.0199 ± 0.0005	0.0341 ± 0.0008
8	0.0267 ± 0.0007	0.0470 ± 0.0008
10	0.0334 ± 0.0005	0.0589 ± 0.0006

Table S19: Solubility of N_2 in pure MEG at $T = 373.15$ K computed using MC simulations reported in this work.

P /[bar]	Mole fraction of N_2
10	0.00093 ± 0.00002
16	0.00146 ± 0.00006
50	0.0045 ± 0.0001
100	0.0084 ± 0.0002

Comparison with experimental data from literature

In this section, a comparison between solubilities of CO_2 measured in this work, from MC simulations, and from other experimental works[10,15,16] is carried out. In Figure S2, shows the loadings of CO_2 at $T = 333$ K as well as at two different temperatures ($T = 323$ K, and $T = 343$ K) from a study by Wise et al.[15] Figure S2 shows that the experimental loadings of CO_2 in MEG at 333 K of this work are higher than experimental loadings reported by Serpa et al.,[16] and Wise et al.[15] The differences between our experimental measurements and that of Serpa et al.,[16] and Wise et al.[15] are larger as the pressure increases. Also, Figure S2 shows that solubilities from MC simulations are higher when compared to experimental measurements from Serpa et al.,[16] and Wise et al.[15]

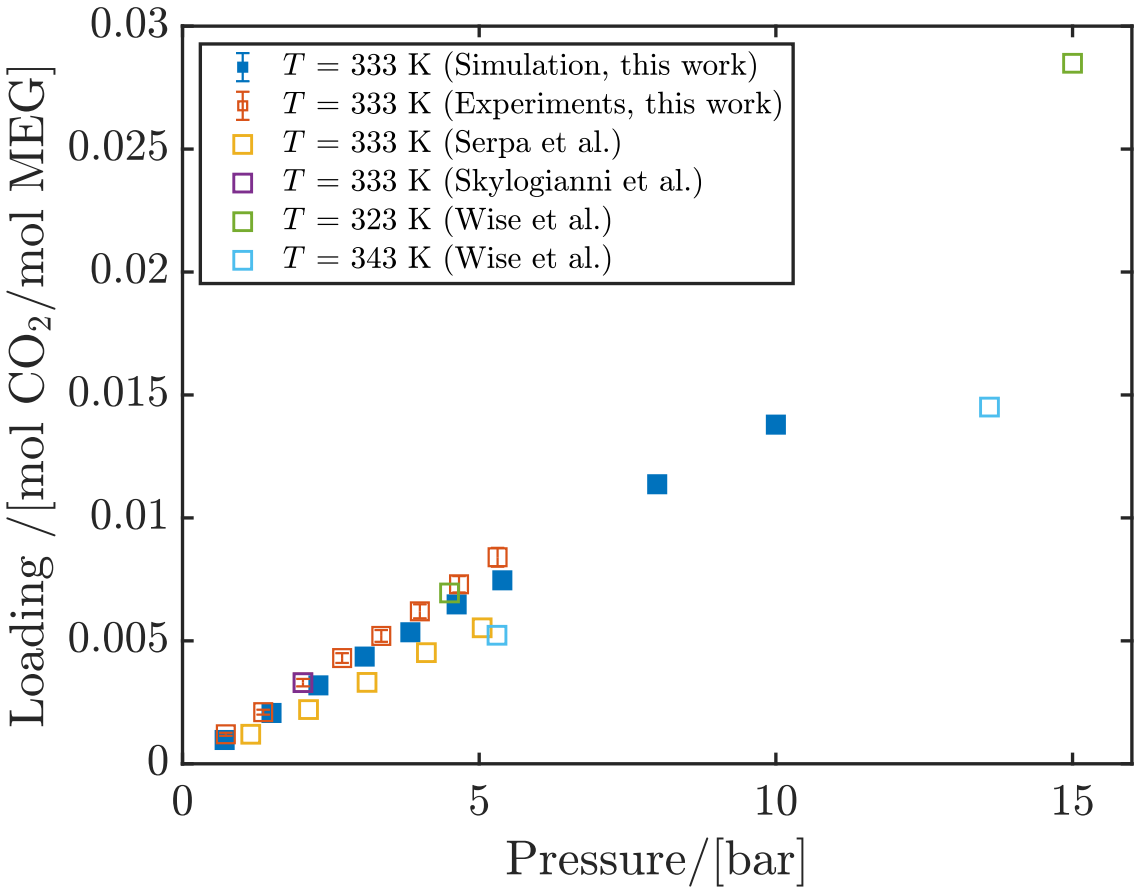

Figure S2: Absorption isotherm of CO_2 in MEG. Closed symbols are solubilities using MC simulations and open symbols are experimental results of this work, from Skylogianni et al.,[10] Serpa et al.,[16] and Wise et al.[15]

References

(1) Stubbs, J. M.; Potoff, J. J.; Siepmann, J. I. Transferable potentials for phase equilibria. 6. United–atom description for ethers, glycols, ketones, and aldehydes. *J. Phys. Chem. B* **2004**, *108*, 17596–17605.

(2) Martin, M. G.; Siepmann, J. I. Transferable potentials for phase equilibria. 1. United–atom description of n–alkanes. *J. Phys. Chem. B* **1998**, *102*, 2569–2577.

(3) Frenkel, D.; Smit, B. *Understanding molecular simulation: from algorithms to applications*, 2nd ed.; Academic press: London, UK, 2002; Vol. 1.

(4) Allen, M. P.; Tildesley, D. J. *Computer simulation of liquids*, 2nd ed.; Oxford University Press, 2017.

(5) Potoff, J. J.; Siepmann, J. I. Vapor–liquid equilibria of mixtures containing alkanes, carbon dioxide, and nitrogen. *AIChE Journal* **2001**, *47*, 1676–1682.

(6) Shah, M. S.; Tsapatsis, M.; Siepmann, J. I. Development of the transferable potentials for phase equilibria model for hydrogen sulfide. *J. Phys. Chem. B* **2015**, *119*, 7041–7052.

(7) Kristóf, T.; Liszi, J. Effective intermolecular potential for fluid hydrogen sulfide. *J. Phys. Chem. B* **1997**, *101*, 5480–5483.

(8) Skylogianni, E.; Wanderley, R. R.; Austad, S. S.; Knuutila, H. K. Density and Viscosity of the Nonaqueous and Aqueous Mixtures of Methyldiethanolamine and Monoethylene Glycol at Temperatures from 283.15 to 353.15 K. *J. Chem. Eng. Data* **2019**, *64*, 5415–5431.

(9) Wanderley, R. R.; Pinto, D. D. D.; Knuutila, H. K. Investigating opportunities for water-lean solvents in CO_2 capture: VLE and heat of absorption in water-lean solvents containing MEA. *Sep. Purif. Technol.* **2020**, *231*, 115883.

(10) Skylogianni, E.; Perinu, C.; Gamerosa, B. Y. C.; Knuutila, H. K. Carbon Dioxide solubility in mixtures of methyldiethanolamine with monoethylene glycol, monoethylene glycol–water, water and triethylene glycol. *J. Chem. Thermodyn.* **2020**, 106176.

(11) Wanderley, R. R.; Ponce, G. J. C.; Knuutila, H. K. Solubility and Heat of Absorption of CO_2 into Diisopropylamine and N, N–Diethylethanolamine Mixed with Organic Solvents. *Energy Fuels* **2020**, *34*, 8552–8561.

(12) Jou, F.; Deshmukh, R. D.; Otto, F. D.; Mather, A. E. Vapor–Liquid Equilibria of H_2S and CO_2 and Ethylene Glycol At Elevated Pressures. *Chem. Eng. Commun.* **1990**, *87*, 223–231.

(13) Galvão, A. C.; Francesconi, A. Z. Solubility of methane and carbon dioxide in ethylene glycol at pressures up to 14 MPa and temperatures ranging from (303 to 423) K. *J. Chem. Thermodyn.* **2010**, *42*, 684–688.

(14) Xu, H.; Zhang, C.; Zheng, Z. Solubility of hydrogen sulfide and carbon dioxide in a solution of methyldiethanolamine mixed with ethylene glycol. *Ind. Eng. Chem. Res.* **2002**, *41*, 6175–6180.

(15) Wise, M.; Chapoy, A. Phase Behavior of CO_2 in Monoethylene Glycol between 263.15–343.15 K and 0.2–40.3 MPa: An Experimental and Modeling Approach. *J. Chem. Eng. Data* **2017**, *62*, 4154–4159.

(16) Serpa, F. S.; Vidal, R. S.; Filho, J. H. A.; Nascimento, J. F. d.; Ciambelli, J. R. P.; Figueiredo, C. M. S.; Salazar-Banda, G. R.; Santos, A. F.; Fortuny, M.; Franceschi, E., et al. Solubility of carbon dioxide in ethane-1, 2-diol–water mixtures. *J. Chem. Eng. Data* **2013**, *58*, 3464–3469.